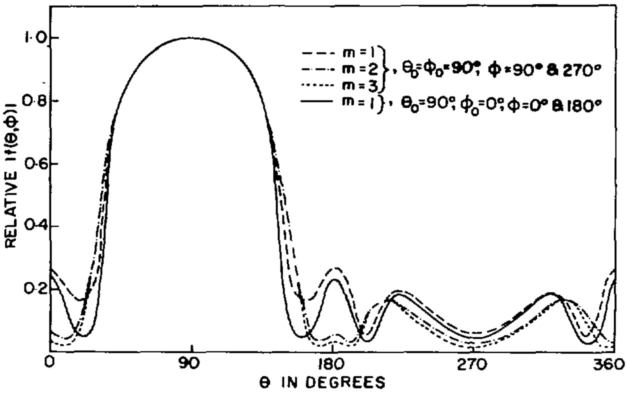

Fig. 2. Vertical radiation patterns for directive continuous spiral antenna array.

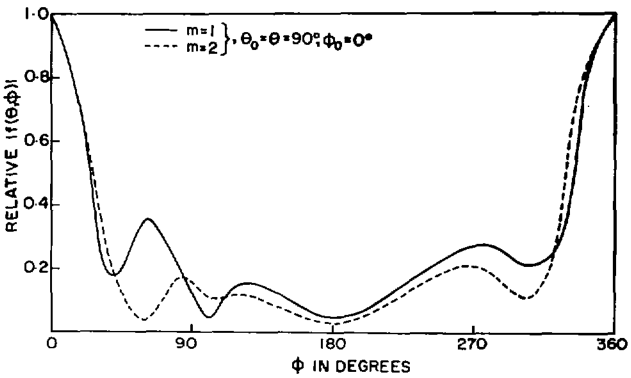

Fig. 3. Horizontal radiation patterns for directive continuous spiral antenna array.

Again from the Bessel's functions properties,

$$\exp\left[\frac{jk_0\zeta}{2}\cos(p\omega-\xi)\right]=\sum_{r=-\infty}^{+\infty} j^r J_r\left(\frac{\zeta k_0}{2}\right)\exp\{jr(p\omega-\xi)\}$$

$$\exp\left[\frac{jk_0\zeta}{2}\cos(q\omega-\xi)\right]=\sum_{s=-\infty}^{+\infty} j^s J_s\left(\frac{\zeta k_0}{2}\right)\exp\{js(q\omega-\xi)\} \tag{12}$$

where r and s are dummies. Substituting the values of the two functions of (12), the final expression for $f(\theta,\phi)$ can be written as

$$\begin{aligned} f(\theta,\phi) &= J_0^2(\zeta k_0/2) - \frac{J_0(\zeta k_0/2)J_2(\zeta k_0/2)}{\pi}\,\frac{2m\sin 2\xi}{m^2-1/16} \\ &\quad + j\left[\frac{J_0(\zeta k_0/2)J_1(\zeta k_0/2)}{\pi}\left\{\frac{4m\sin\xi-\cos\xi}{2(m^2-1/16)}\right\}\right. \\ &\quad + \frac{J_1(\zeta k_0/2)J_2(\zeta k_0/2)}{2\pi}\left\{\frac{3\cos\xi-4m\sin\xi}{m^2-9/16}\right. \\ &\quad \left.\left. + \frac{\cos 3\xi - 12\sin 3\xi}{9m^2-1/16}\right\}\right]. \end{aligned} \tag{13}$$

In deriving (13), only the significant terms have been retained and other terms, which can be made very small by a proper choice of k_0a, have been neglected [3].

Now from (13), the modulus of $f(\theta,\phi)$ can be calculated for different desired values of θ_0 and ϕ_0 according to suitable choice of array dimension and wavelength used.

Numerical Computations and Discussion of Results

Theoretically the vertical and the horizontal radiation patterns have been considered for different values of m. The value of $k_0a = 5$ is taken to ensure the validity of (13) in all the computations.

The vertical radiation patterns have been computed by taking $\theta_0 = \phi_0 = 90°$ and $\phi = 90°$ and $270°$ for three values of $m = 1, 2$, and 3. The variation of $|f(\theta,\phi)|$ with θ is shown in Fig. 2. In another case, it is assumed that $\phi_0 = 0°$, $\theta_0 = 90°$, $\phi = 0°$ and $180°$, and $m = 1$. This radiation pattern is also exhibited in Fig. 2 for comparison. It is observed that a flat maximum is obtained for all the cases and the beamwidth angle is about 100°. The plane $\theta = 90°$ is a plane of mirror symmetry obviously because the array has been placed in this plane. In the graph for $m = 1$ and $\phi = 90°$ and 270°, two secondary lobes appear with successively decreasing intensities. The intensity of the first sidelobe is about one-fourth of that of the main directional beam. A flat plataeu of low intensity is observed between 220° and 320°. For $m = 2$ and 3, the patterns are similar in nature except that the sidelobe levels decrease with the increase of m. The nature of the two curves for $m = 1$, shown in Fig. 2 is almost alike except for some changes in magnitude.

The horizontal patterns showing the variation of $|f(\theta,\phi)|$ with ϕ are shown in Fig. 3. The main direction $\theta_0 = \theta = 90°$, $\phi_0 = 0°$ for $m = 1$ and 2 is considered. For $m = 1$, the beamwidth angle is about 36° which is much less than the corresponding beamwidth angle of the vertical pattern. A very large flat plataeu with a low intensity is observed. The pattern for $m = 2$ is similar to the pattern for $m = 1$ with reduced sidelobe levels. Further reduction in sidelobe level is possible by increasing the number of spiral turns. As the spiral is not a symmetrical figure, no symmetry is obtained in either of the two horizontal patterns. One may thus conclude that the sidelobe levels of the horizontal patterns can be reduced significantly by using more turns of the spiral.

From Figs. 2 and 3, it is clear that the horizontal radiation patterns are sharper than the corresponding vertical patterns having the same number of spiral turns.

References

[1] W. L. Curtis, "Spiral antennas," *IRE Trans. Antennas Propagat.*, vol. AP-8, pp. 298–306, May 1960.

[2] K. K. Dey and P. Khastgir, "Radiation from a plane spiral antenna array," *Proc. Inst. Radio Elec. Eng., Aust.*, vol. 32, no. 9, pp. 349–351, Sept. 1971.

[3] ——"Radiation from a continuous spiral antenna array," *Proc. Inst. Radio Elec. Eng. Aust.*, vol. 32, No. 9, pp. 351–353, Sept. 1971.

[4] R. E. Collin and F. C. Zucker, *Antenna Theory*, Part I. New York: McGraw-Hill, 1969, ch. 5, sec. 5.6.

A Portable Coaxial Collinear Antenna

B. B. BALSLEY and WARNER L. ECKLUND

***Abstract*—A novel collinear antenna constructed of coaxial cable with inner- and outer-conductors interchanged at half-wavelength intervals is described. A 26-element antenna of this type has been constructed and evaluated. Design criteria presented allow extension to the use of coaxial cable of different types in a variety of radio/radar arrays.**

Introduction

There are a variety of situations in present-day HF or VHF radio/radar applications that require a directional antenna which is lightweight, portable, easily-erected, and reasonably inexpensive. This communication describes a simple antenna that satisfies these requirements. The antenna is constructed of a series of half-wavelengths of coaxial cable that have been connected together by electrically interchanging the inner- and outer-conductors at each junction. The resulting antenna has the physical form of a

Manuscript received January 17, 1972; revised February 11, 1972.
The authors are with the Environmental Research Laboratories, National Oceanic and Atmospheric Administration, U. S. Department of Commerce, Boulder, Colo. 80302.

single long section of flexible coaxial line, while electrically it is composed of a number of collinear half-wave dipoles fed in phase. In practice, beamwidths of 1 to 15° are obtainable.

Description

Although the length, operating frequency, and cable size for a specific antenna can vary widely depending upon particular requirements, we will describe here a 49.8 MHz 26-element coaxial collinear antenna mounted one wavelength above ground and constructed of RG-8 coaxial cable. The antenna has been specifically designed for a radar system for both transmission and reception, and will handle peak pulse power in excess of 100 kW, provided the average power rating of the cable is not exceeded.

A schematic diagram of the complete 26-element coaxial collinear antenna system is shown in Fig. 1. The antenna is connected to a 3/8″ Nylon messenger line by a series of slip-rings that are attached to the cable at regular intervals as indicated in inset A of Fig. 1. As indicated in inset B of Fig. 1, the antenna is fed at the two outer-conductors of the center elements. Feeding can be accomplished either directly by a two-wire transmission line or by a quarter-wave transformer and a balun as shown.

Fig. 2(a) shows the details of interchanging the inner- and outer-conductors at each half-wave section of cable. Each half-wave section is cut to 0.67 × free-space length to compensate for the propagation velocity in the cable. Note that the outer braid has been peeled back about 1″ from each cable end to expose the polyethylene insulation. Fig. 2(b) shows a connection similar to the one shown in Fig. 2(a), after it has been weather sealed. The sealing process consists of first coating the entire connection with silicon sealant and then covering the connection with heat-shrink tubing. The resulting seal is weather resistant and sufficiently strong to withstand temporary tension well in excess of 300 lb. All of the connections are treated in the same manner except for the two end elements, which are left unconnected and are sealed in the same manner as the others.

Antenna Pattern

The radiation pattern of an even number n of collinear half-wave dipoles fed in phase with a nonuniform amplitude distribution which is symmetric about the center elements may be expressed [1] as

$$E_T = \frac{2\cos((\pi/2)\sin\theta)}{\cos(\theta)} \sum_{k=0}^{k=(n-2)/2} A_k \cos\left(\frac{2k+1}{2}\psi\right) \qquad (1)$$

where E_T represents the field intensity of the total array; A_k is the amplitude of the kth element set measured from the center of the array; θ is measured from a line normal to the antenna axis; and ψ is expressed in terms of $\beta d = (2\pi/\lambda)d$, i.e., the distance d between elements expressed in radians

$$\psi = \beta d \sin(\theta). \qquad (2)$$

The element spacing d is $0.67\lambda/2$, owing to the velocity factor of the cable. The value of A_k is approximately determined by the cable loss/dipole at the operating frequency. For RG-8 at 50 MHz, A_k is given by

$$A_k = \frac{1}{(1.0233)}. \qquad (3)$$

A normalized theoretical radiation pattern obtained from (1) for a 26-element antenna is shown in Fig. 3 by a dashed line. Note that the theoretical beamwidth to half-power points of the 26-element antenna is 5.6°. Note also that the theoretical 15.5-dB sidelobe level of the tapered array is 2.3 dB below that expected for a uniformly fed system. The tapering is due to the cable loss/dipole A_k, and even greater sidelobe reduction could be obtained by using higher loss cable, although the beamwidth would be increased.

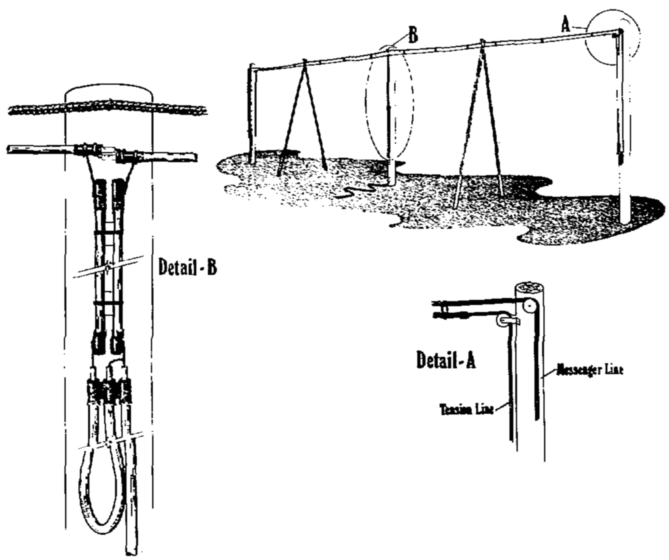

Fig. 1. Sketch of 26-element coaxial collinear antenna mounted on three poles, showing feeding and tensioning arrangements. Details of the 3/8″ nylon messenger line and the polyethylene rings used to connect to the antenna are shown in inset A. Inset B shows the antenna-feed arrangement consisting of balun and a quarter-wave matching transformer. All electrical connections shown are normally weatherproofed.

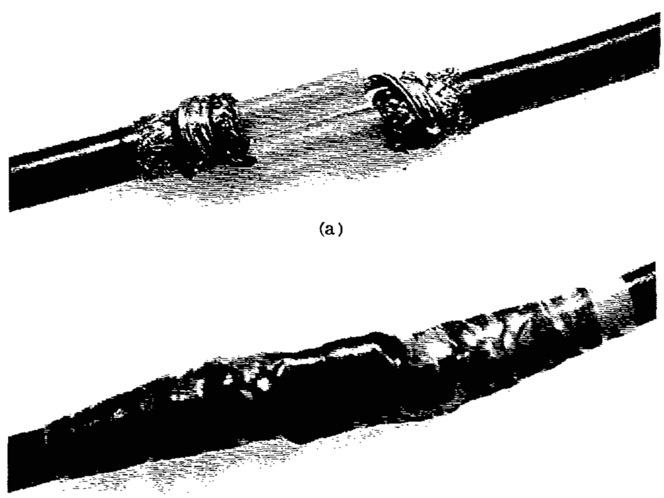

(a)

(b)

Fig. 2. Details of connections between adjacent elements. (a) Interconnection of inner- and outer-conductors before sealing. (b) Connection which has been weather-sealed.

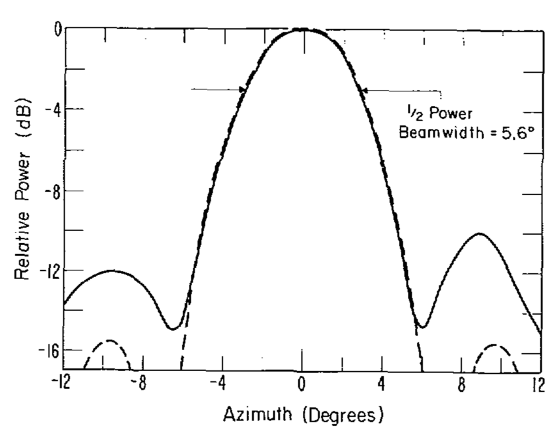

Fig. 3. Theoretical and measured radiation patterns for 26-element antenna. Theoretical curve is shown by dashed line, while measured curve is solid.

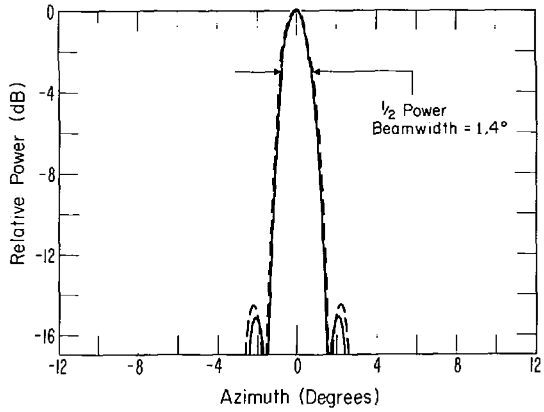

Fig. 4. Theoretical and measured radiation patterns for collinear broadside array of four 26-element antennas. Dashed curve refers to theoretical pattern, while solid curve depicts measured values. Total beamwidth is 1.4°.

A pattern measured by flying a transmitting source through the beam is shown in the same figure by a solid line. The computed and measured curves are seen to be in substantial agreement except for the sidelobe levels where the differences are probably attributable to the uneven terrain where the antenna was located.

In addition to the preceding antenna system, four 26-element antennas were connected as a linear array having a total of 104 collinear elements. The four feedlines were connected together by an appropriate matching network, and the pattern was determined both theoretically and by actual measurement. The results are shown in Fig. 4. Again the theoretical and measured patterns are in good agreement, indicating a half-power beamwidth of 1.4°. The sidelobe levels for the four-section array are down by about 15 dB with respect to the main beam maximum (the pattern for this array was measured over much flatter terrain so that the sidelobe levels are probably more accurate).

Admittance and Bandwidth

The admittance versus frequency characteristic of the unmatched antenna is shown in Fig. 5(a). The data show the antenna to be slightly inductive at all frequencies around the design frequency. Matching was accomplished by connecting a small (50 pf) capacitance across the antenna terminals, and by adjusting the quarter-wave transformer spacing.

With regard to antenna bandwidth limitations, the degradation of the antenna system as a function of frequency can occur in two separate ways: 1) the feed-point admittance can change from its design value, or 2) the antenna pattern can vary from the designated pattern. Either of these two factors can be used to define a usable antenna bandwidth, provided that the maximum allowable variations are specified.

For the present purpose, the admittance variation can be expressed in terms of the voltage standing-wave ratio (VSWR), since the maximum allowable variation is determined by the ability of the transmitter to feed a mismatched system. The VSWR for the matched 26-element antenna is shown in Fig. 5(b). Assuming a maximum permissible VSWR of 2.0, the resulting bandwidth is about 1.0 MHz.

A similar procedure can be followed with regard to the antenna pattern variation. In this case the degradation is basically determined by the total number of wavelengths between the feed point and the end of the antenna. This is due to the fact that a signal whose frequency is slightly different from the design frequency will appear at an adjacent element slightly shifted from the desired phase; the effect is cumulative so that the end element is the most affected. This results in a distorted antenna pattern. If we define the usable bandwidth of the antenna as that frequency deviation from the design frequency which results in a phase variation on the end element of not more than $\pi/6$ radians, the bandwidth may be

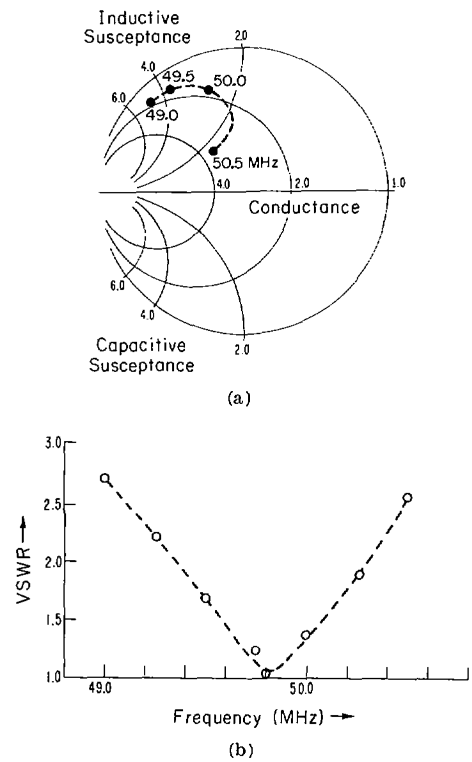

Fig. 5. (a) Admittance [normalized to $(300\ \Omega)^{-1}$] versus frequency for 26-element antenna. (b) VSWR versus frequency for same antenna after impedance matching for VSWR = 1.0 at 49.8 MHz design frequency.

expressed as

$$\text{bandwidth} = \frac{2f_0}{3n + 1} \quad (4)$$

where both the bandwidth and the design frequency f_0 are expressed in MHz, and n is the number of half-wave elements in the complete antenna. Using (4) the 50 MHz 26-element antenna described here has a bandwidth of about 1.3 MHz.

Conclusions

The coaxial collinear antenna is useful in instances where portability, ease-of-installation, narrow beamwidth, and cost are major factors. For example, the 5°, 26-element antenna described herein, including the 3/8″ messenger line, weighs less than 30 lb and can be stowed in a 2′ × 2′ × 1′ container for shipment. The total construction costs amount to only about three times the cost of the coaxial cable, and installation time (assuming the support poles are installed) is less than one hour.

The 26- and 104-element arrays described in this report have measured patterns in good agreement with theory, and can be easily matched to ordinary coaxial line. Design criteria presented here enable ready extension to the use of coaxial cable of different types in linear arrays of widely varying dimensions.

Acknowledgment

The idea of interchanging the inner- and outer-conductors of coaxial transmission line to make an antenna was originally suggested a number of years ago [2]–[4]. This concept has since been used in at least two separate instances [5], [6]. The latter reference describes the 18 432-element incoherent-scatter antenna of the Jicamarca Radar Observatory, near Lima, Peru.

We are indebted to D. R. Askey and P. E. Johnston for help in the antenna construction, and to A. M. Gray, P. H. Jones, and M. M. Larsh of the NOAA Space Environment Monitoring Station, Anchorage, Alaska, and to R. A. Greenwald for help in measuring and mounting the 26- and 104-element arrays. Low-loss flexible coaxial feed line used in the 104-element array was kindly provided by W. K. Klemperer from NOAA's Space Environment Laboratory, Boulder, Colo. K. Neal, also of the Space Environment Laboratory, provided the time-shared computer program used for impedance transformation.

References

[1] J. D. Kraus, *Antennas.* New York: McGraw-Hill, 1950, cf. ch. 4.
[2] P. V. Handel and W. Pfister, "Ausbreitung der Mikrostrahlen," Zentrale für technischwissenschaftliches Berichtswesen über Luftfahrtforschung, Germany, Res. Rep. FB338, May 6, 1935.
[3] S. I. F. Fayard, Au brevet d'invention No. 782.801 (1ns addition), Perfectionnements aux antennas de T.S.F., Ministry of Commerce and Industry, France, patent published Sept. 12, 1935.
[4] H. B. Hollman, *Physik und Technik der Ultrakurzen Wellen.* Berlin, Germany: Springer, 1936. (See "Konzentrische Rohrleitung als Obserwellenantenna," after Pfister in Fig. 84, pp. 74 of vol. II, "Die ultrakurzen Wellen in der Technik.")
[5] H. A. Wheeler, "A vertical antenna made of transposed sections of coaxial cable," in 1956 *IRE Conv. Rec.*, vol. 4, pt. 1.
[6] G. R. Ochs, "The large 50 Mc/s dipole array at Jicamarca Radar Observatory," Nat. Bur. Stand, Boulder, Colo., Rep. 8772, Mar. 5, 1965.

The Loop Antenna with Director Arrays of Loops and Rods

J. APPEL-HANSEN

Abstract—Experiments indicate that the gain of a Yagi–Uda antenna arrangement depends only upon the phase velocity of the surface wave traveling along the director array and not to any significant extent upon the particular forms of the director elements.

In the common Yagi–Uda antenna, rod directors are usually used. According to Ehrenspeck and Poehler [1], the phase velocity of the surface wave traveling along the array of rod directors can be used as the design criterion for maximum gain. This seems to indicate that the magnitude of the gain depends only on the phase velocity of the surface wave and not on the particular form of the director elements. The purpose of the present investigation is to verify whether an array of short-circuited loops in front of the loop antenna provides the same gain as an array of rod directors.

In Fig. 1, the geometry of the directive loop array antenna is shown. It consists of a feeding loop, a reflector loop, and an array of equispaced loop directors of equal diameter. The feeding loop is a shielded loop made of coaxial cable of 4-mm diameter. The reflector and director loops are made of 1.25-mm aluminum plate. The difference between inner and outer radius of these flat-plate loops is 1 cm. When a radius of a loop is indicated, it designates the average radius of the loop in question. The measurements were carried out in a radio anechoic chamber at 650 MHz. The gain over an isotropic radiator was measured.

The measurements started with an optimization of the diameter of the shielded feeding loop. A gain of 3.4 dB was obtained at a circumference of $ka_f = 1.10$, where $k = 2\pi/\lambda$ is the wavenumber, λ is the wavelength, and a_f the radius of the feeding loop.

After this optimization, a reflector of the same diameter as the feeding loop was added. By optimizing several times in turns, the spacing between feeding loop and reflector loop, the diameter of the reflector, and the diameter of the feeding loop, an optimum gain of 7.8 dB was obtained. This compares well with results obtained by Ito *et al.* [2].

In front of the feeding arrangement so obtained, a director array of short circuited loops with an equidistance of 0.2λ was placed. The length of this array was varied in steps of 0.4λ from 0λ to 4λ. For each length, the gain was measured as a function of the radius a_d of the director loops. In Fig. 2, as an example, the gain as a function of ka_d for an array 2λ long is shown. It is seen that a maximum gain of 13.8 dB was measured. In Fig. 3, the maximum gain obtained in this manner by varying the director loop diameter for the different array lengths l is shown. The same measurement procedure was carried out for a director array consisting of 2 mm wire loops. In completion it should be mentioned that the results do not change when the loop directors are open circuited in one or both of their current minima.

Manuscript received February 3, 1972.
The author is with the Laboratory of Electromagnetic Theory, The Technical University, Lyngby, Denmark.

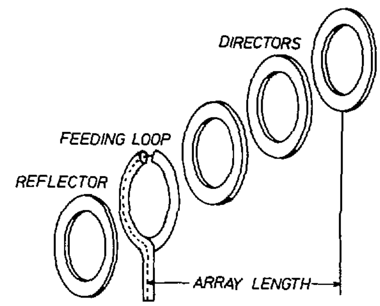

Fig. 1. Directive loop array antenna.

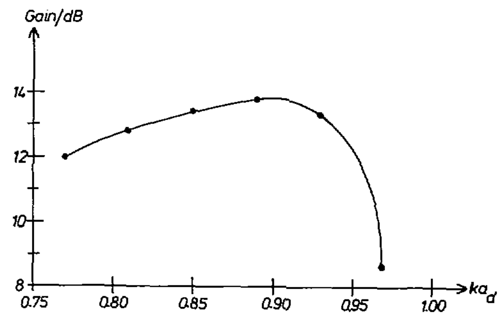

Fig. 2. Gain as function of ka_d. Array length 2λ.

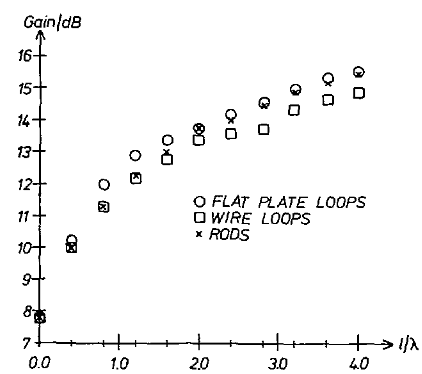

Fig. 3. Gain as function of array length.

Following this, an array of rod directors with equispacing 0.2λ was placed in front of the feeding arrangement. This time, by varying the length of the rod directors, the maximum gain for several array lengths between 0.4λ and 4.0λ was measured. For comparison between the three types of director elements, the results for the rod directors are also shown in Fig. 3.

From Fig. 3, we may conclude that there is no more than about 1-dB difference between the gain of the various types of director elements. For the array lengths considered the flat-plate loops seem to be more effective for lengths less than 2λ, whereas the wire loops are the least effective for lengths larger than 2λ. Due to the small difference between the results, the experiments seem to confirm that the maximum gain only depends upon the phase velocity of the surface wave and not upon the particular form of the director elements.